Composite scaffold obtained by electro-hydrodynamic technique for infection prevention and treatment in bone repair

Javier Aragón, Sergio Feoli, Silvia Irusta, Gracia Mendoza

PII: S0378-5173(18)30895-0
DOI: https://doi.org/10.1016/j.ijpharm.2018.12.002
Reference: IJP 17962

To appear in: *International Journal of Pharmaceutics*

Received Date: 31 August 2018
Revised Date: 30 November 2018
Accepted Date: 1 December 2018

Please cite this article as: J. Aragón, S. Feoli, S. Irusta, G. Mendoza, Composite scaffold obtained by electro-hydrodynamic technique for infection prevention and treatment in bone repair, *International Journal of Pharmaceutics* (2018), doi: https://doi.org/10.1016/j.ijpharm.2018.12.002

Composite scaffold obtained by electro-hydrodynamic technique for infection prevention and treatment in bone repair

Javier Aragón[a,b], Sergio Feoli[a,b], Silvia Irusta[a,b,c,*], Gracia Mendoza[a,b,*]

[a]Department of Chemical Engineering, Aragon Institute of Nanoscience (INA), University of Zaragoza, Campus Rio Ebro-Edificio I+D, C/ Mariano Esquillor S/N, 50018 Zaragoza, Spain

[b]Aragon Health Research Institute (IIS Aragon), 50009 Zaragoza, Spain

[c]Networking Research Center on Bioengineering, Biomaterials, and Nanomedicine, CIBER-BBN, 28029 Madrid, Spain

Corresponding authors: *Email addresses: sirusta@unizar.es (S. Irusta), gmmenc@unizar.es (G. Mendoza). Department of Chemical Engineering, Aragon Institute of Nanoscience, University of Zaragoza, 50018 Zaragoza, Spain. Phone: +34 876555437; +34 876554342.

ABSTRACT

Bone infection is a devastating condition resulting from implant or orthopaedic surgery. Therapeutic strategies are extremely complicated and may result in serious side effects or disabilities. The development of enhanced 3D scaffolds, able to promote efficient bone regeneration, combined with targeted antibiotic release to prevent bacterial colonization, is a promising tool for the successful repair of bone defects. Herein, polymeric electrospun scaffolds composed of polycaprolactone (PCL) nanofibres decorated with poly(lactic-co-glycolic acid) (PLGA) particles loaded with rifampicin were fabricated to achieve local and sustained drug release for more efficient prevention and treatment of infection. The release profile showed an initial burst of rifampicin in the first six hours, enabling complete elimination of bacteria. Sustained and long-term release was observed until the end of the experiments (28 days), facilitating a prolonged effect on the inhibition of bacterial growth, which is in agreement with the common knowledge concerning the acidic degradation of the microparticles. In addition, bactericidal effects against gram negative (*Escherichia coli*) and gram positive (*Staphylococcus aureus*) bacteria were demonstrated at concentrations of released rifampicin up to 58 ppm after 24 h, with greater efficacy against *S. aureus* (13 ppm vs 58 ppm for *E. coli*). Cell morphology and cytocompatibility studies highlighted the suitability of the fabricated scaffolds to support cell growth, as well as their promising clinical application for bone regeneration combined with prevention or treatment of bacterial infection.

Keywords: Electrospinning; Polymeric scaffold; Polycaprolactone; Poly(lactic-co-glycolic acid); Rifampicin; Bone infection

1. Introduction

Bone repair mediated by scaffold or substitute implantation is one of the most useful strategies in traumatology, orthopaedics, and maxillofacial surgery. Autologous bone graft implantation has been considered the main technique to successfully repair bone defects. However, in clinical practice, invasiveness at the donor site and inability to absorb large grafts are problematic (Dong et al., 2014; Ghassemi et al., 2018; Weisz and Errico, 2000).

Bone infection resulting from implantation or orthopaedic surgery is a serious complication characterized by an inflammatory reaction and bone destruction (Arciola et al., 2012; Rumian et al., 2016). Although implant-associated infections in orthopaedics are relatively uncommon (2-5%), implant replacement and possible resulting disabilities have a high impact on the patient's quality of life and result in economic and clinical burden (Darouiche, 2004).

Most bone infections are caused by staphylococcal species, with *Staphylococcus aureus* being the most prevalent, though other microorganisms (i.e. *Pseudomonas aeruginosa*, *Escherichia coli*) may also be involved (Andrés et al., 2018; Arciola et al., 2012; Johnson and García, 2015). Intervention to prevent these infections is critical in the first hours after surgery, as they often originate during the surgical procedure. Rifampicin (RFP) is effective against staphylococcal infections and efficient for treatment at any bacterial growth stage (i.e. exponential, stationary, intracellular) (Frippiat et al., 2004; Sanz-Ruiz et al., 2017; Trampuz and Widmer, 2006). Furthermore, RFP is also one of the most effective first-line drugs for the treatment of tuberculosis and its bone-related effects (i.e. osteomyelitis, bone destruction) (Yuan et al., 2015).

Oral and systemic administration of antibiotics for the prophylaxis or treatment of bone infections can be ineffective due to low delivery and permeation of antibiotics into bone

and the possible presence of bacterial biofilms (Flores et al., 2016; Furustrand Tafin et al., 2015; Zhu et al., 2015). Therefore, the need for local treatments, characterized by an initial burst of antibiotics followed by a sustained release of an adequate drug dose to prevent any further infection, seems to be imperative to successfully treat these pathologies (Gimeno et al., 2015; Rumian et al., 2016).

Recently, the development of novel materials as scaffolds for bone regeneration has increased to provide therapeutic options for challenging bone pathologies, such as those resulting from trauma or tumour resection (Ghassemi et al., 2018). These scaffolds are designed as templates to mimic the extracellular matrix, providing adequate mechanical and architectural features as well as osteoconductive and osteoinductive properties. Furthermore, the addition of biologically active molecules, such as growth factors or drugs, enhances their therapeutic potential for bone regeneration (Dorati et al., 2017; Porter et al., 2009).

Several materials have been reported to promote bone repair. Specially, synthetic polymers, such as polylactic acid (PLA), polyglycolic acid (PGA), poly(lactic-co-glycolic acid) (PLGA), or polycaprolactone (PCL), facilitate control of the physico-chemical and mechanical features of the synthesised scaffolds (Dorati et al., 2017; Ghassemi et al., 2018; Liu and Ma, 2004). In particular, electrospun PCL fibres have been previously reported as highly mimetic of the extracellular matrix and promising for bone regeneration strategies, combining the versatility and simplicity of the electrospinning technique with the biocompatibility of PCL and its degradation products (Aragon et al., 2017; Baker et al., 2016; Porter et al., 2009; Song et al., 2013). Conversely, PLGA, an FDA-approved polymer, is widely used in biomedical applications, mainly in drug delivery and tissue engineering, due to its high

biocompatibility and hydrolytic degradation to its biocompatible constituents PLA and PGA (Makadia and Siegel, 2011).

Antibiotic-loaded scaffolds for the *in situ* treatment of bone infection may provide targeted drug delivery and sustained release, resulting in sustained enhancement of osteogenic properties for the successful regeneration of bone. Furthermore, scaffolds eliminate the need for long-term oral and intravenous systemic multidrug administration, which results in toxic side effects, low delivery to the target site, and low patient adherence to treatment (Johnson and García, 2015; Yang et al., 2016; Yuan et al., 2015; Zhu et al., 2011). RFP-loaded PCL electrospun scaffolds showed an initial burst release, with 50% of the loaded drug remaining entrapped within the scaffold. Despite only 50% release, *P. aeruginosa* and *Staphylococcus epidermidis* growth was hindered compared to growth in response to unloaded scaffolds (Ruckh et al., 2012). Furthermore, studies (Yang et al., 2016) have demonstrated that chitosan grafted to printed scaffolds composed of PLGA and hydroxyapatite decreased bacterial adhesion and showed osteoconductive properties.

The aim of this work was to synthesize and characterize a drug delivery system consisting of PCL electrospun nanofibres with RFP-PLGA electrosprayed particles within the scaffold to promote bone repair while preventing infection. The bactericidal ability of the synthesized electrospun material was assessed *in vitro* against gram positive (*S. aureus*) and gram negative (*E. coli*) bacteria, and the cytocompatibility was assessed in human osteoblast 3D cultures.

2. Materials and methods

2.1. Materials

N,N-dimethylformamide (DMF; ≥99.8%), dichloromethane (DCM; ≥99.8%), acetic acid (≥99%), dimethyl sulfoxide (DMSO; ≥99.8%), PCL with an average molecular

weight of 80,000 Da, RFP (≥97%), and 3-(3,4-dimethylthiazol-2-yl)-2,5-diphenyltetrazoliumbromide (MTT; ≥98%) were purchased from Sigma-Aldrich (Spain). PLGA 50:50 ester terminated with 38,000-54,000 Da molecular weight was purchased from Evonik Industries (Spain). Sodium dodecyl sulfate (SDS) and Triton X-100 were obtained from Bio-Rad (USA). *Escherichia coli* S17 was kindly gifted by Dr. J. A. Aínsa, while *Staphylococcus aureus* (ATCC®25923) was purchased from Ielab (Spain). Trypticasein soy broth (TSB) and trypticasein soy agar (TSA) were acquired from Conda-Pronadisa (Spain). Osteoblast growth medium (OGM) and human osteoblasts (HOBs) were obtained from PromoCell (Germany). Trypsin-EDTA and Dulbecco's phosphate-buffered saline (DPBS) were obtained from Biowest (France).

2.2. PLGA particles production

PLGA particles were prepared by electrospray using a Yflow 2.2.D-500 electrospinner (Electrospinning Machines/R&D Microencapsulation, Spain). The following parameter settings were investigated to obtain the microparticles: polymer concentration (5, 7.5 and 10% w/w); feeding flow rate (0.5 and 1.0 mL/h); and distance from the tip to the collector (15 and 30 cm). PLGA (0.50, 0.77, and 1.05 g) was dissolved in 10 mL of DMF to obtain final concentrations of 5, 7.5 and 10%, respectively (w/w). RFP (55, 85, and 117 mg) was added to each PLGA solution at 10% (w/w) and stirred overnight at 4 °C. The solution was loaded into a 10 mL plastic syringe and fed through a needle connected to a positive power supply. The tip of the needle was fixed 15 or 30 cm above a rotating collection drum. The negative voltage power supply was connected to the collector, which was rotated at 100 rpm. Flow rates of 0.5 and 1.0 mL/h were investigated to optimize PLGA particle production.

2.3. Electrospun scaffold production

PCL membranes decorated with PLGA particles loaded with RFP were also produced using a Yflow 2.2.D-500 electrospinner (Electrospinning Machines/R&D Microencapsulation, Spain) following the protocol described in previous studies (Aragón et al., 2018). Two needles were used to obtain the PCL fibres (needle 1) and to electrospray the PLGA-RFP particles (needle 2). Through needle 1, a 7.5% PCL (w/w) in a DCM-DMF (1:1) mixture was fed at 1.5 mL/h, while a PLGA-RFP solution was fed at 1.0 mL/h through needle 2. Both needles were connected to a positive power supply at a voltage of 18.7 kV. The tips of the needles were fixed at 18 cm (needle 1) and 15 cm (needle 2) above a rotating collection drum at 100 rpm. The negative voltage power supply (-3.3 kV) was connected to the collector. The production process required 8 h.

2.4. Scaffold characterization

The morphology of PLGA particles and electrospun scaffolds was analyzed under a scanning electron microscope (SEM; Field Emission Scanning Electron Microscope CSEM-FEG INSPECT 50, FEI, US). Particle and fibre diameters were measured by Image J software (Version 1.48f, NIH, US).

Mechanical properties of the composite scaffolds were determined at room temperature using a uniaxial Instron test machine (Instron, US) with video extensometer 5548 (1 KN load cell, 1 mm/min). Five samples per membrane were cut into 50 mm × 5 mm strips and subjected to a tensile test. A full-scale load of 20 N and maximum extension of 100 mm were used.

The encapsulation efficiency (EE) of RFP was analyzed by absorbance measurement at 334 nm using a calibration curve prepared from a RFP standard at 50 ppm in DMF using a microplate reader (Multimode Synergy HT Microplate Reader; Biotek, US).

Approximately 10-20 mg of PCL-PLGA-RFP scaffold (five replicas were analyzed) was placed in 1 mL of DMF and agitated for 3 h at 4 °C to extract the loaded RFP.

The EE was calculated with Eq. 1, taking into account the exact weight of the scaffolds analyzed:

$$EE = \frac{RFP\ measured\ amount}{RFP\ theoretical\ amount} \times 100 \qquad (1)$$

The theoretical amount was calculated based on the RFP added to the electrospray solution.

The *in vitro* release of RFP from loaded electrospun scaffolds (15-20 mg) was performed at 37 °C (Heater Memmert, Germany) in DPBS (1.5 mL). At scheduled time intervals (from 1 h to 28 days), all DPBS were harvested and an equal volume of fresh DPBS was added back to the vessels. The collected samples (five replicates per time point) were stored at -20 °C until analysis.

To determine the RFP concentration, three aliquots (150 μL) per sample were added to a 96-well plate to measure the absorbance. The RFP calibration curves in DPBS were prepared across the range of 0-50 ppm and measured in triplicate

2.5. Bactericidal tests

To evaluate the antimicrobial efficiency of the fabricated materials, the minimum inhibitory concentration (MIC) and minimum bactericidal concentration (MBC) of the PCL-PLGA-RFP electrospun scaffolds were determined against *E. coli S17* as a gram negative model, and *S. aureus* as a gram positive infective model.

Antibacterial activities of the RFP-loaded electrospun scaffolds against *E. coli* and *S. aureus* were studied using ASTM E-2180 ("ASTM E2180 - 18 Standard Test Method for Determining the Activity of Incorporated Antimicrobial Agent(s) In Polymeric or Hydrophobic Materials," n.d.), as it is the recommended methodology to quantitatively determine the antibacterial activity of hydrophobic materials. Briefly, an overnight

stationary growth phase of bacteria in TSB was diluted in sterile TSA solution at 40 °C to obtain a starting bacterial concentration of 10^5 colony forming units per milliliter (CFU/mL). The inoculated TSA was placed in a 12-well plate (2 mL per well). The electrospun scaffolds were sterilized on both sides by UV-irradiation for 1 h and weighed to obtain RFP concentrations ranging from 0.5 to 90 ppm, considering the total amount of RFP loaded in the scaffolds. Then, these scaffolds were placed in the 12-well plate on the bacteria-inoculated TSA. After incubation (37 °C, 24 h), the samples were collected in 10 mL of sterile TSB, sonicated in an ultrasonic bath (50 kHz) for 1 min, then vortex-mixed for 1 min to accurately determine the bacterial growth. Subsequently, the samples were serially diluted in PBS and spot-plated on TSA plates (four replicates per sample). Viable bacterial colonies were counted after overnight incubation at 37 °C and compared to those obtained from the control sample (PCL-PLGA electrospun scaffolds without RFP). Each experiment was performed in triplicate and the results are reported as mean ± S.D.

2.6. Cell attachment and morphology

Electrospun scaffolds (15 mm diameter, surface area 1.54 cm^2) were sterilized on both sides by UV-irradiation for 1 h and successively soaked with an OGM culture medium for 1 h to avoid floating. HOBs were grown in the OGM culture medium in a 5% CO_2 atmosphere at 37 °C. The culture medium was removed and 10 µL of cell suspension (3.2 x 10^6 cells/mL) was seeded on the top region of the scaffolds. To promote cell adhesion to the scaffold, the samples were incubated for 1 h (5% CO_2, 37 °C) followed by addition of 500 µL of OGM. The seeded scaffolds were cultured for 3, 7, 14, and 28 days, renewing the culture medium every 2-3 days. In addition, 2D cultures (HOBs seeded on 24-well plates) were also run as cell growth and proliferation control samples.

SEM was used to observe the morphology of the attached cells to the electrospun scaffolds. At the time points indicated above, the seeded scaffolds were washed with DPBS and fixed in a 4% paraformaldehyde solution (Affymetrix, US) for 30 min at room temperature. After fixation, the samples were washed with DPBS and distilled water, air-dried, and sputter-coated with a thin platinum layer prior to visualization by SEM (Field Emission Scanning Electron Microscope CSEM-FEG INSPECT 50, FEI, US).

Confocal analysis was performed to observe the cytoskeleton protein distribution of actin (Alexa Fluor™ 546 Phalloidin; Molecular Probes, US) after 3, 7, 14, and 28 days of cell culture. Seeded scaffolds were rinsed with DPBS and fixed with 4% paraformaldehyde solution for 15 min. Then, samples were permeabilized in ice-cold acetone (-20 °C, 5 min), air-dried, and rinsed with DPBS. Triton X-100 (0.5%) was added to the samples for blocking (30 min) with 5% normal donkey serum (NDS; Jackson ImmunoResearch Europe Ltd, UK). After blocking, actin staining (1:200; Alexa Fluor™ 546 Phalloidin; Molecular Probes, US) was performed for 30 min at room temperature. The scaffolds were then washed with DPBS and incubated with 8 μM anthraquinone dye (DRAQ5; eBiocence, US) for 30 min at room temperature to stain the cellular nuclei. Finally, samples were washed, mounted, and visualized under a confocal laser scanning microscope (Leica TCS SP2, Leica, Germany).

2.7. In vitro cytotoxicity studies

The cytotoxicity of the seeded electrospun scaffolds with and without RFP was determined by the 3-(3,4-dimethylthiazol-2-yl)-2,5-diphenyltetrazoliumbromide (MTT) test at the time points described above (3-28 days) (Morelli et al., 2014). In brief, an MTT solution (5 mg/mL in DPBS) was diluted in OGM (final concentration 0.5 mg/mL), added to the seeded scaffolds at the time points described above, and

incubated for 4 h at 37 °C and 5% CO_2. The cell medium was discarded and the insoluble formazan crystals obtained were dissolved by addition of SDS (sodium dodecyl sulfate; Bio-Rad, US) solution (100 mg/mL in DMSO and 0.6% of acetic acid). Aliquots (100 µL) were transferred to a 96-well plate and the absorbance was read at 570 nm in a Synergy HT microplate reader (Biotek, US). Results were expressed as mean ± SD of the total absorbance of the samples analyzed in triplicate.

2.8. Statistical analysis

All data are reported as mean ± SD. For fibre and particle diameter, n = 100 were studied. For confocal analysis, more than 50 planes per region and three regions per sample were evaluated. MTT determination was performed in triplicate and three measurements were performed per experiment (9 sets of data). Statistical analysis of data was performed using the Student-Newman-Keuls t-test and ANOVA (Statgraphics® Centurion XV statistical software, StatPoint Technologies, Inc., US). Statistically significant differences were considered when $p \leq 0.01$.

3. Results and discussion

3.1. Characterization of composite scaffolds

Composite scaffolds were fabricated by electrospinning to obtain PCL fibres decorated with PLGA-RFP particles, which were synthesized by electrospraying.

Different conditions were evaluated to determine their effects on PLGA-RFP particle fabrication and to optimize their synthesis. These conditions included the polymer concentration (5, 7.5 and 10% w/w), flow rate (0.5 and 1.0 mL/h), and distance from the tip to the collector (15 and 30 cm). The results obtained regarding particle diameter and morphology, and the percentage of size distribution, as functions of the different synthesis conditions evaluated, are detailed in Table SI1 and also shown in Figures 1, SI1, and SI2.

Modification of synthesis conditions resulted in low variation of the mean particle diameter, producing microparticles with mean diameters around 1 μm. However, the highest mean diameter (2 μm) was obtained when the polymer concentration was also the highest (10%), though these particles had the highest size dispersion percentage (57.8%) (Table SI1). The best results were obtained when the polymer concentration was 7.5% (w/w), the electrospray flux was 1.0 mL/h, and the distance from the tip to the collector was 15 cm. As shown in the SEM images (Fig. 1 and Fig. SI1), PLGA-RFP particles fabricated at the optimized conditions exhibited homogeneous morphology and the lowest percentage of dispersion of mean diameter (27.82%; Table SI1 and Fig. SI2). The histogram depicted a group of particles with diameters in the range of 0.8-2.0 μm, with a mean diameter of 1.3 ± 0.4 μm, though some larger particles were present (~3 μm diameter). However, use of the same flux and tip-collector distance with the lowest polymer concentration (5%) did not produce well-defined particles (Fig. SI1) and a mean diameter could not be calculated (Fig. SI2).

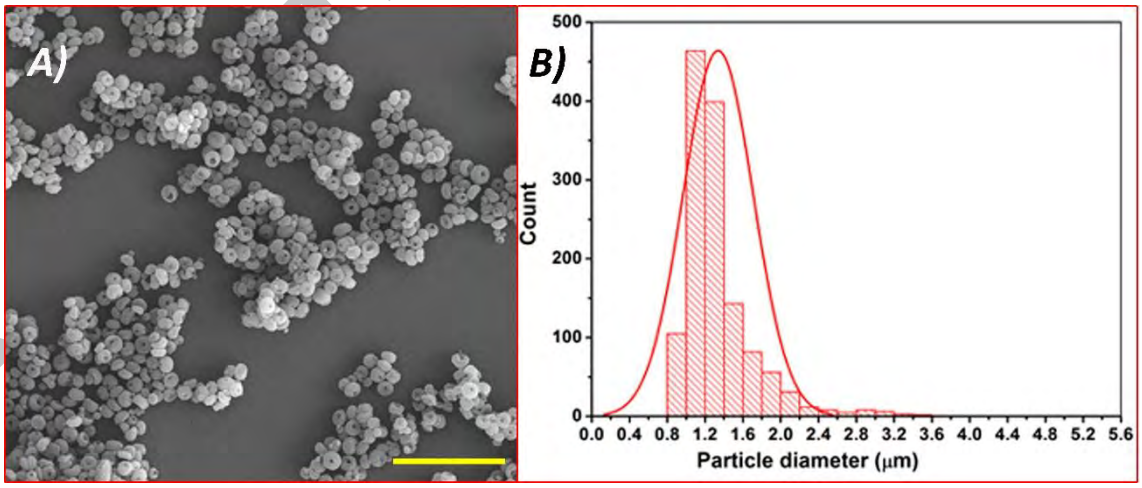

Fig. 1. a) SEM image of the electrosprayed PLGA-RFP particles obtained at a flux of 1.0 mL/h, 7.5% PLGA concentration and a distance of 15 cm from the tip to the collector, scale bar = 10 μm.; b) histogram of the particle size distribution.

After particle synthesis optimization, the composite scaffolds were fabricated by simultaneous electrospray-electrospinning (Fig. 2). The optimized scaffolds showed homogenous morphology and particle distribution. PCL nanofibres showed a mean diameter of 477 ± 246 nm (Fig. 2A), while fibres with PLGA-RFP particles attached had a mean diameter of 678 ± 381 nm (Fig. 2B). Attached PLGA-RFP particles had a mean diameter of 1.1 ± 0.2 μm (19% of size dispersion). The fabricated multifunctional scaffold was characterized by a porous network with a large surface area-to-volume ratio, which is an essential condition for cell adhesion and proliferation and, therefore, adequate for bone regeneration. Absorbance measurements determined an RFP concentration loaded onto the synthesized scaffold of 2 ± 1 wt% (encapsulation efficiency of 57 ± 26%).

Bone scaffolds are expected to have enough mechanical resistance to support cell expansion and tissue regeneration, and should be able to withstand manipulation. The mechanical properties of the scaffolds with and without RFP are described in Table 1, showing no significant differences between the types of scaffolds. These results are in agreement with previous studies regarding PCL electrospun scaffolds for bone regeneration applications (Heydari et al., 2017).

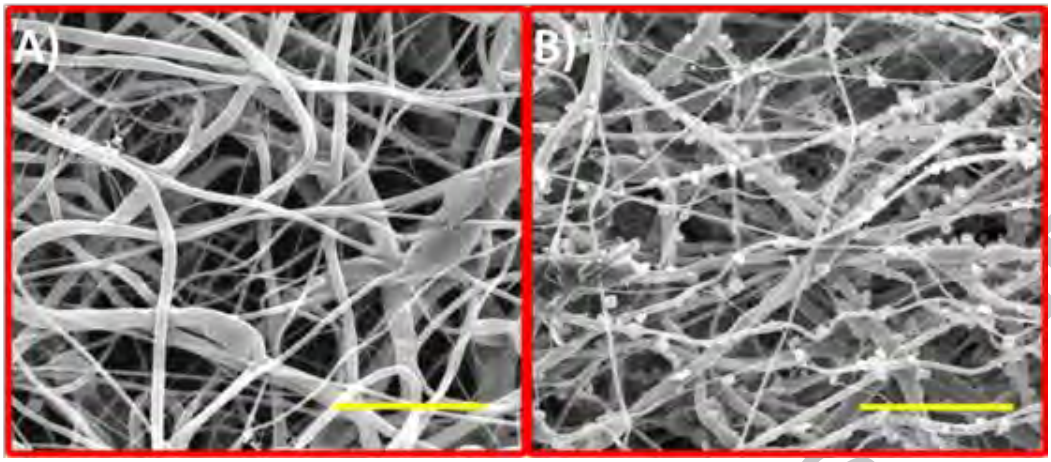

Fig. 2. SEM images of electrospun PCL fibres (A) and the PCL scaffolds decorated with the electrosprayed PLGA-RFP particles (B) at a flux of 1.0 mL/h, 7.5% PLGA concentration and a distance of 15 cm from the tip to the collector. Scale bar = 10 μm.

Table 1. Mechanical properties of the electrospun scaffolds.

Condition	PCL/PLGA	PCL/PLGA-RFP
Tensile strength (MPa)	2.4 ± 0.6	2.6 ± 0.7
Young´s Module (MPa)	9.0 ± 4.0	8.0 ± 2.0
Strain at break (%)	140.0 ± 20.0	150.0 ± 30.0

The release profile of RFP was evaluated until the end of the experiments (28 days; Fig. 3). Antibiotic release from the composite scaffolds displayed a sharp initial burst within the first 6 h, with the majority released within the first hour, followed by sustained release until 28 days. In contrast, previous studies evaluating electrospun PCL scaffolds directly loaded with RFP showed drug release up to 8 h (Ruckh et al., 2012). In our study, at the end of the experiments (28 days), the total RFP released was 82% of the loaded drug in the scaffolds. The initial burst and the subsequent long-term sustained release is applicable to bone infection-control, allowing adequate regeneration of bone

while avoiding the impairment of bone repair (Gimeno et al., 2015; Rumian et al., 2016).

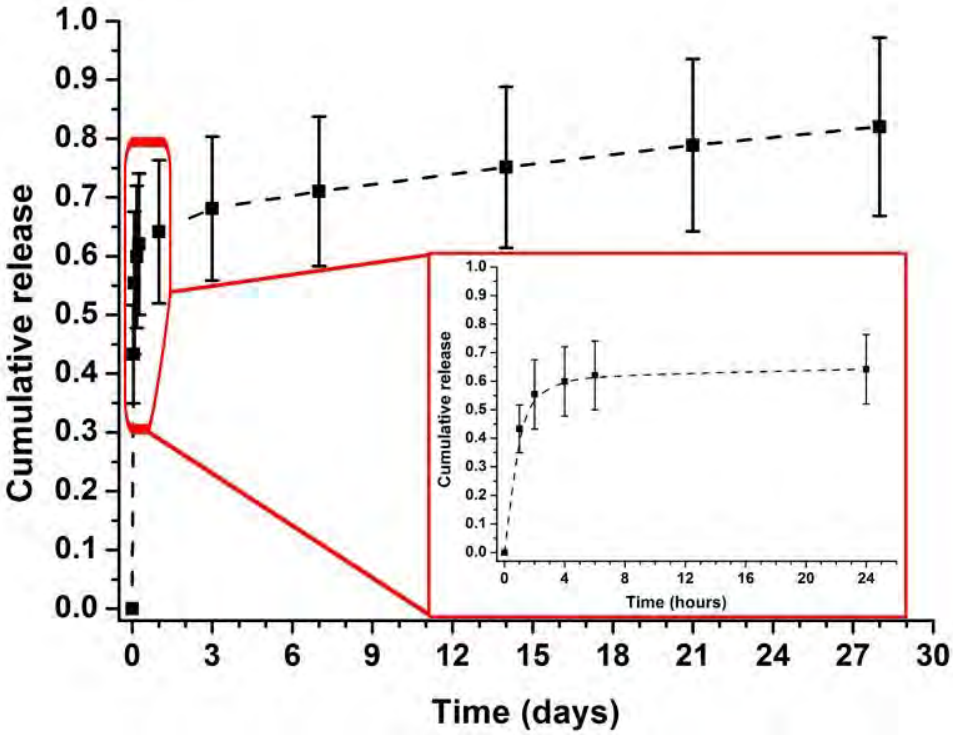

Fig. 3. Rifampicin release profile obtained from the composite scaffolds until the end of the experiments (28 days). The inset details the drug release for the first 24 h.

3.2. *MIC and MBC determination*

The bactericidal effects of the fabricated composite scaffolds were tested against *E. coli S17* (gram negative) and *S. aureus* (gram positive). The scaffold masses evaluated were calculated to evaluate RFP concentrations in the range of 0.5-90 ppm (0.5, 1, 5, 10, 15, 20, 25, 30, 45, 60, 75, and 90 ppm).

The effects observed were significantly different between gram negative and gram positive bacteria, with MIC values of 75 ppm in *E. coli* and 5 ppm in *S. aureus*, which corresponds to 48 ppm and 3 ppm of released RFP in 24 h, respectively. These differences were consistent with MBC values, in which 90 ppm of loaded RFP (58 ppm

of released RFP in 24 h) was needed to completely eliminate *E. coli*, whereas 20 ppm (13 ppm of released RFP in 24 h) was enough to eradicate *S. aureus*. These values are higher than reported RFP serum levels (1-6 μg/mL) after administration of the maximum recommended therapeutic dosage (450-600 mg/day) for the treatment of bone infection and tuberculosis (Mehta et al., 2001; Roth, 1984; van Ingen et al., 2011). Therefore, the fabricated scaffolds were able to successfully release a therapeutically effective amount of RFP directly into the target tissue, avoiding acid degradation and kidney and liver clearance of RFP after oral administration. Furthermore, side effects resulting from oral administration are not relevant with local administration (Singh et al., 2013). Moreover, according to our results, the required concentration of RFP to eradicate bacteria (13-58 ppm released in 24 h) was also achieved in the release assays as reported above (96-116 ppm in 24 h), highlighting the potential of these scaffolds to achieve their clinical purpose.

RFP is a wide antibacterial spectrum antibiotic with a bactericidal mechanism of action mediated by inhibition of bacterial RNA polymerase. Different sensitivities of gram negative and gram positive bacteria to RFP treatment have been previously demonstrated, and were not attributed to differences in polymerases, but to the better penetrability of RFP through gram positive cell walls than through gram negative outer membranes (Wehrli, 1983).

3.3. In vitro cell studies

Human osteoblasts were seeded onto RFP-loaded composite scaffolds to evaluate cell adhesion, proliferation and morphology by SEM and confocal microscopy (Figs. 4 and 5, Video SI). Both types of scaffolds assayed (PCL-PLGA and PCL-PLGA-RFP) showed adhesion and homogeneous distribution of HOBs on the scaffold surface. Cell proliferation was also demonstrated as the surface was completely covered by HOBs at

the end of the experiments (28 days), though PCL-PLGA-RFP scaffolds had lower cell density on their surface, pointing to a possible toxicity mediated by RFP.

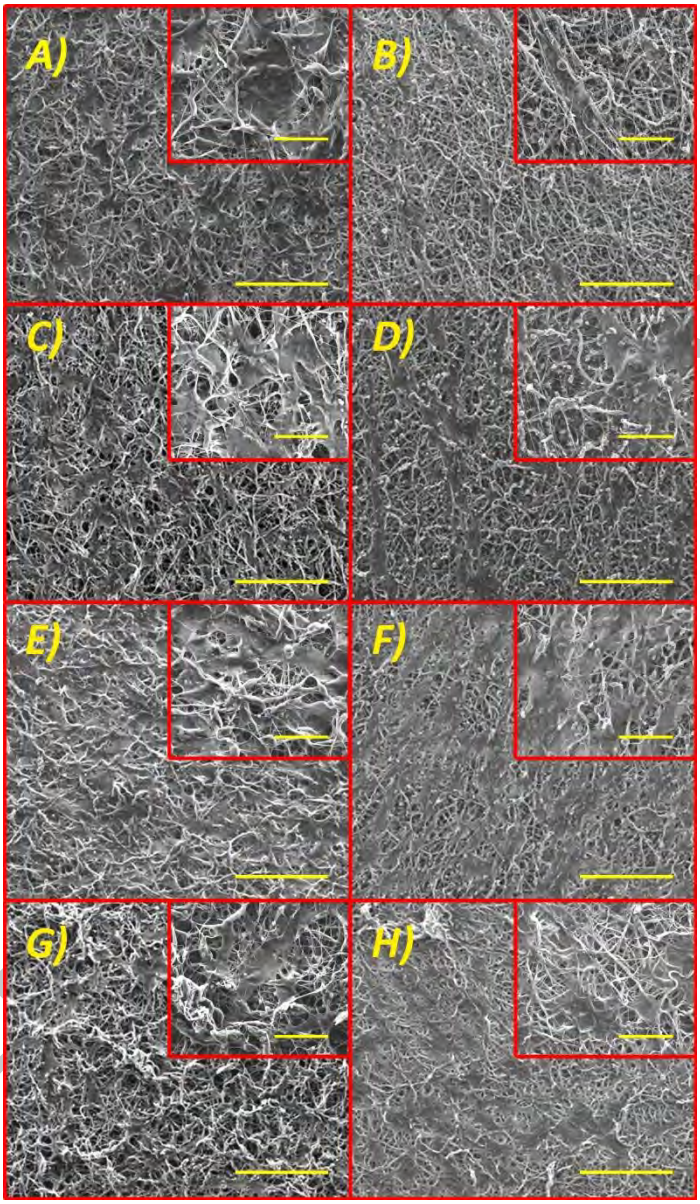

Fig. 4. Cell proliferation on rifampicin-loaded scaffolds (B, D, F, H) and on PCL-PLGA scaffolds (A, C, E, G) at different time points: 3 days (A, B), 7 days (C, D), 14 days (E, F) and 28 days (G, H). Cell structure is apparent when the fibre morphology is blurred due to cell growth on the fibres. Scale bar = 100 μm; Inset scale bar = 30 μm.

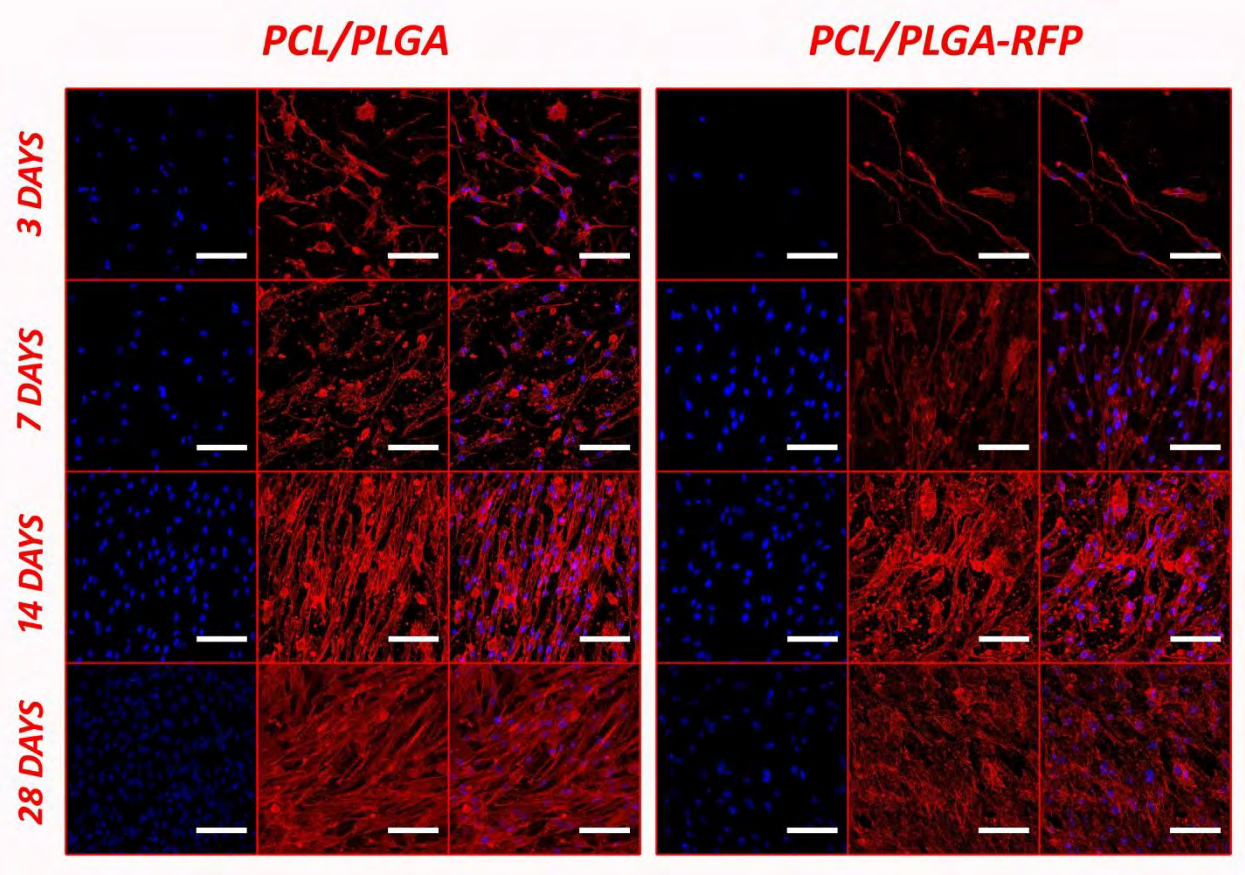

Fig. 5. Cell morphology and proliferation on PCL-PLGA scaffolds (left panel) and on rifampicin-loaded PCL-PLGA (RFP) scaffolds (right panel) at the time points studied. Nuclei are stained in blue (left column in each panel) and cytoskeleton in red (medium column in each panel). The last column in each panel displays the merge images. Scale bar = 100 μm.

MTT assays (Fig. 6) confirmed the growth pattern of HOBs on RFP-loaded scaffolds, showing slightly lower viability when the antibiotic was present, in accordance with previous studies that reported decreased cell viability after treatment with free RFP at similar drug concentrations (≤100 μg/mL vs 96-148 μg/mL RFP released from our scaffolds) (Yuan et al., 2015). At the end of the experiments (28 days), cell viability was not different between 2D cultures and 3D cultures on RFP-loaded scaffolds, whereas 3D cell cultures exerted higher viability percentages, highlighting the effect of RFP on cell

proliferation and the 3D effect on cell growth. However, the effect of RFP may not be considered relevant to cell growth as the scaffold surface was completely covered by HOBs after 28 days, pointing to their suitability for bone regeneration purposes.

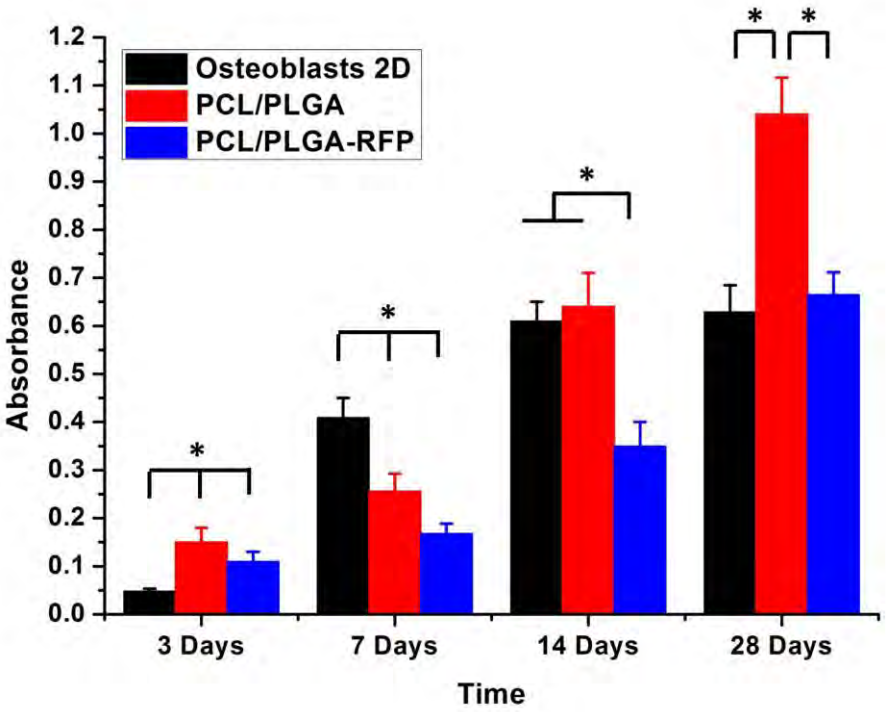

Fig. 6. Cell viability of human osteoblasts seeded on a 2D system and on the two types of scaffolds assayed, PCL-PLGA and rifampicin (RFP)-loaded scaffolds, at the time points studied. Data are represented as absorbance values (mean ± SD; n = 9). Statistically significant differences between groups were considered when $p \leq 0.01$.

4. Conclusions

A polymeric multifunctional scaffold was developed combining electrospun PCL nanofibres with electrosprayed RFP-PLGA microparticles for bone repair and prevention or treatment of bone infection. The RFP scaffold load was 2 ± 1 wt% with an encapsulation efficiency of 57%. The synthesized scaffold showed a porous network

with a homogeneous distribution of RFP-PLGA microparticles (around 1 μm diameter). An initial burst of RFP release was followed by sustained release until the end of the experiments, reaching 82% release of the loaded drug. This release profile is suitable for clinical application, as bone infection is initially controlled by the burst, with sustained release providing prophylaxis to avoid bone reinfection. Microbiological studies supported the potential of the fabricated scaffolds for bone infection treatment, as concentrations ≤58 ppm were able to eliminate *E. coli* and *S. aureus* and are in the range of the serum therapeutic dosages clinically recommended. Moreover, HOBs seeded on these scaffolds proliferated and completely colonized the surface. We thus have demonstrated that our scaffolds are potential candidates for bone repair when infection may impair regeneration of the tissue, though further studies regarding the *in vivo* efficacy of the fabricated scaffolds against bone infection should be conducted to fully understand their suitability for the intended clinical application.

Acknowledgments

The authors would like to thank Ministerio de Economia y Competitividad, CTQ2014-52384-R (Spain) for the financial support. CIBER-BBN is an initiative funded by the VI National R&D&i Plan 2008-2011, Iniciativa Ingenio 2010, Consolider Program, CIBER Actions and financed by the Instituto de Salud Carlos III (Spain) with assistance from the European Regional Development Fund. J.A. acknowledges support from Education, Audiovisual and Culture Executive Agency (EU-EACEA) within the EUDIME-"Erasmus Mundus Doctorate in Membrane Engineering" program (5th Ed.). We acknowledge the LMA-INA and Microscopy and Cell Culture Core Units from IACS/IIS Aragon for their instruments and expertise.

Declaration of interests

None.

Appendix A. Supplementary data

Supplementary data associated with this article can be found, in the online version, at XXXX.

References

Andrés, N.C., Sieben, J.M., Baldini, M., Rodríguez, C.H., Famiglietti, Á., Messina, P. V, 2018. Electroactive Mg2+-Hydroxyapatite Nanostructured Networks against Drug-Resistant Bone Infection Strains. ACS Appl. Mater. Interfaces 10, 19534–19544. https://doi.org/10.1021/acsami.8b06055

Aragon, J., Navascues, N., Mendoza, G., Irusta, S., 2017. Laser-treated electrospun fibers loaded with nano-hydroxyapatite for bone tissue engineering. Int. J. Pharm. 525, 112–122. https://doi.org/10.1016/j.ijpharm.2017.04.022

Aragón, J., Salerno, S., De Bartolo, L., Irusta, S., Mendoza, G., 2018. Polymeric electrospun scaffolds for bone morphogenetic protein 2 delivery in bone tissue engineering. J. Colloid Interface Sci. 531, 126–137. https://doi.org/10.1016/j.jcis.2018.07.029

Arciola, C.R., Campoccia, D., Speziale, P., Montanaro, L., Costerton, J.W., 2012. Biofilm formation in Staphylococcus implant infections. A review of molecular mechanisms and implications for biofilm-resistant materials. Biomaterials 33, 5967–5982. https://doi.org/10.1016/J.BIOMATERIALS.2012.05.031

ASTM E2180 - 18 Standard Test Method for Determining the Activity of Incorporated Antimicrobial Agent(s) In Polymeric or Hydrophobic Materials [WWW Document], n.d. URL https://www.astm.org/Standards/E2180 (accessed 7.29.18).

Baker, S.R., Banerjee, S., Bonin, K., Guthold, M., 2016. Determining the mechanical properties of electrospun poly-ε-caprolactone (PCL) nanofibers using AFM and a novel fiber anchoring technique. Mater. Sci. Eng. C 59, 203–212.

https://doi.org/10.1016/j.msec.2015.09.102

Darouiche, R.O., 2004. Treatment of Infections Associated with Surgical Implants. N. Engl. J. Med. 350, 1422–1429. https://doi.org/10.1056/NEJMra035415

Dong, J., Zhang, S., Liu, H., Li, X., Liu, Y., Du, Y., 2014. Novel alternative therapy for spinal tuberculosis during surgery: reconstructing with anti-tuberculosis bioactivity implants. Expert Opin. Drug Deliv. 11, 299–305. https://doi.org/10.1517/17425247.2014.872625

Dorati, R., DeTrizio, A., Modena, T., Conti, B., Benazzo, F., Gastaldi, G., Genta, I., 2017. Biodegradable Scaffolds for Bone Regeneration Combined with Drug-Delivery Systems in Osteomyelitis Therapy. Pharmaceuticals 10, 96. https://doi.org/10.3390/ph10040096

Flores, C., Degoutin, S., Chai, F., Raoul, G., Hornez, J.-C., Martel, B., Siepmann, J., Ferri, J., Blanchemain, N., 2016. Gentamicin-loaded poly(lactic-co-glycolic acid) microparticles for the prevention of maxillofacial and orthopedic implant infections. Mater. Sci. Eng. C 64, 108–116. https://doi.org/10.1016/j.msec.2016.03.064

Frippiat, F., Meunier, F., Derue, G., 2004. Place of newer quinolones and rifampicin in the treatment of Gram-positive bone and joint infections. J. Antimicrob. Chemother. 54, 1158–1158. https://doi.org/10.1093/jac/dkh451

Furustrand Tafin, U., Betrisey, B., Bohner, M., Ilchmann, T., Trampuz, A., Clauss, M., 2015. Staphylococcal biofilm formation on the surface of three different calcium phosphate bone grafts: a qualitative and quantitative in vivo analysis. J. Mater. Sci. Mater. Med. 26, 130. https://doi.org/10.1007/s10856-015-5467-6

Ghassemi, T., Shahroodi, A., Ebrahimzadeh, M.H., Mousavian, A., Movaffagh, J., Moradi, A., 2018. Current Concepts in Scaffolding for Bone Tissue Engineering.

Arch. bone Jt. Surg. 6, 90–99.

Gimeno, M., Pinczowski, P., Pérez, M., Giorello, A., Martínez, M.Á., Santamaría, J., Arruebo, M., Luján, L., 2015. A controlled antibiotic release system to prevent orthopedic-implant associated infections: An in vitro study. Eur. J. Pharm. Biopharm. 96, 264–271. https://doi.org/10.1016/j.ejpb.2015.08.007

Heydari, Z., Mohebbi-Kalhori, D., Afarani, M.S., 2017. Engineered electrospun polycaprolactone (PCL)/octacalcium phosphate (OCP) scaffold for bone tissue engineering. Mater. Sci. Eng. C 81, 127–132. https://doi.org/10.1016/j.msec.2017.07.041

Johnson, C.T., García, A.J., 2015. Scaffold-based anti-infection strategies in bone repair. Ann. Biomed. Eng. 43, 515–28. https://doi.org/10.1007/s10439-014-1205-3

Liu, X., Ma, P.X., 2004. Polymeric scaffolds for bone tissue engineering. Ann. Biomed. Eng. 32, 477–86.

Makadia, H.K., Siegel, S.J., 2011. Poly Lactic-co-Glycolic Acid (PLGA) as Biodegradable Controlled Drug Delivery Carrier. Polymers (Basel). 3, 1377–1397. https://doi.org/10.3390/polym3031377

Mehta, J.B., Shantaveerapa, H., Byrd, R.P., Morton, S.E., Fountain, F., Roy, T.M., 2001. Utility of rifampin blood levels in the treatment and follow-up of active pulmonary tuberculosis in patients who were slow to respond to routine directly observed therapy. Chest 120, 1520–4.

Morelli, M.B., Amantini, C., Nabissi, M., Liberati, S., Cardinali, C., Farfariello, V., Tomassoni, D., Quaglia, W., Piergentili, A., Bonifazi, A., Del Bello, F., Santoni, M., Mammana, G., Servi, L., Filosa, A., Gismondi, A., Santoni, G., 2014. Cross-talk between alpha1D-adrenoceptors and transient receptor potential vanilloid type 1 triggers prostate cancer cell proliferation. BMC Cancer 14, 921.

https://doi.org/10.1186/1471-2407-14-921

Porter, J.R., Ruckh, T.T., Popat, K.C., 2009. Bone tissue engineering: A review in bone biomimetics and drug delivery strategies. Biotechnol. Prog. 25, 1539–1560. https://doi.org/10.1002/btpr.246

Roth, B., 1984. Penetration of Parenterally Administered Rifampicin into Bone Tissue. Chemotherapy 30, 358–365. https://doi.org/10.1159/000238294

Ruckh, T.T., Oldinski, R.A., Carroll, D.A., Mikhova, K., Bryers, J.D., Popat, K.C., 2012. Antimicrobial effects of nanofiber poly(caprolactone) tissue scaffolds releasing rifampicin. J. Mater. Sci. Mater. Med. 23, 1411–1420. https://doi.org/10.1007/s10856-012-4609-3

Rumian, Ł., Tiainen, H., Cibor, U., Krok-Borkowicz, M., Brzychczy-Włoch, M., Haugen, H.J., Pamuła, E., 2016. Ceramic scaffolds enriched with gentamicin loaded poly(lactide- co -glycolide) microparticles for prevention and treatment of bone tissue infections. Mater. Sci. Eng. C 69, 856–864. https://doi.org/10.1016/j.msec.2016.07.065

Sanz-Ruiz, P., Carbó-Laso, E., Del Real-Romero, J.C., Arán-Ais, F., Ballesteros-Iglesias, Y., Paz-Jiménez, E., Sánchez-Navarro, M., Pérez-Limiñana, M.Á., Vaquero-Martín, J., 2017. Microencapsulation of rifampicin: A technique to preserve the mechanical properties of bone cement. J. Orthop. Res. 36, 459–466. https://doi.org/10.1002/jor.23614

Singh, H., Bhandari, R., Kaur, I.P., 2013. Encapsulation of Rifampicin in a solid lipid nanoparticulate system to limit its degradation and interaction with Isoniazid at acidic pH. Int. J. Pharm. 446, 106–111. https://doi.org/10.1016/j.ijpharm.2013.02.012

Song, W., Yu, X., Markel, D.C., Shi, T., Ren, W., 2013. Coaxial PCL/PVA electrospun

nanofibers: osseointegration enhancer and controlled drug release device. Biofabrication 5, 035006. https://doi.org/10.1088/1758-5082/5/3/035006

Trampuz, A., Widmer, A.F., 2006. Infections associated with orthopedic implants. Curr. Opin. Infect. Dis. 19, 349–356. https://doi.org/10.1097/01.qco.0000235161.85925.e8

van Ingen, J., Aarnoutse, R.E., Donald, P.R., Diacon, A.H., Dawson, R., Plemper van Balen, G., Gillespie, S.H., Boeree, M.J., 2011. Why Do We Use 600 mg of Rifampicin in Tuberculosis Treatment? Clin. Infect. Dis. 52, e194–e199. https://doi.org/10.1093/cid/cir184

Wehrli, W., 1983. Rifampin: Mechanisms of Action and Resistance. Clin. Infect. Dis. 5, S407–S411. https://doi.org/10.1093/clinids/5.Supplement_3.S407

Weisz, R.D., Errico, T.J., 2000. Spinal infections. Diagnosis and treatment. Bull. Hosp. Jt. Dis. 59, 40–6.

Yang, Y., Yang, S., Wang, Y., Yu, Z., Ao, H., Zhang, H., Qin, L., Guillaume, O., Eglin, D., Richards, R.G., Tang, T., 2016. Anti-infective efficacy, cytocompatibility and biocompatibility of a 3D-printed osteoconductive composite scaffold functionalized with quaternized chitosan. Acta Biomater. 46, 112–128. https://doi.org/10.1016/j.actbio.2016.09.035

Yuan, J., Wang, B., Han, C., Lu, X., Sun, W., Wang, D., Lu, J., Zhao, J., Zhang, C., Xie, Y., 2015. In vitro comparison of three rifampicin loading methods in a reinforced porous β-tricalcium phosphate scaffold. J. Mater. Sci. Mater. Med. 26, 174. https://doi.org/10.1007/s10856-015-5437-z

Zhu, M., Li, K., Zhu, Y., Zhang, J., Ye, X., 2015. 3D-printed hierarchical scaffold for localized isoniazid/rifampin drug delivery and osteoarticular tuberculosis therapy. Acta Biomater. 16, 145–155. https://doi.org/10.1016/J.ACTBIO.2015.01.034

Zhu, M., Wang, H., Liu, J., He, H., Hua, X., He, Q., Zhang, L., Ye, X., Shi, J., 2011. A mesoporous silica nanoparticulate/β-TCP/BG composite drug delivery system for osteoarticular tuberculosis therapy. Biomaterials 32, 1986–1995. https://doi.org/10.1016/j.biomaterials.2010.11.025